JSEE Vol. 23, No. 3, 2021 DOI: 10.48303/jsee.2023.1990039.1052

*Research Paper*

# Effect of Seismic Site Response on Damage Distribution in Sarpol-e Zahab City Caused by November 12, 2017 Mw 7.3 Strong Ground Motion: Fooladi Area

**Shima Pakniat[1], Mojtaba Moosavi[2*] and Javad Jalili[2]**

1. M.Sc. Graduate of Earthquake Engineering, Geotechnical Engineering Research Center, International Institute of Earthquake Engineering and Seismology (IIEES), Tehran, Iran
2. Assistant Professor, Geotechnical Engineering Research Center, International Institute of Earthquake Engineering and Seismology (IIEES), Tehran, Iran,
*Corresponding Author; email: moosavi@iiees.ac.ir

**Received:** 20/02/2022
**Revised:** Not Required
**Accepted:** 15/03/2023

## ABSTRACT

*The event of Sarpol-e Zahab with magnitude of 7.3 severely struck the border area of Iran and Iraq in Kermanshah province, leading to catastrophic damages to a wide region, specially Sarpol-e Zahab city. Doubts arouse whether the damage distribution all over the city stemed from the seismic ground response or superficial loose fill material. The issue was explored in this study by especial attention to an area with high damages in Sarpol-e Zahab, called Fooladi. Since the seismic bedrock motion was not available, it was first deconvoluted from the recorded acceleration on the ground surface. Then ground response analysis was conducted at three different locations in Fooladi area, by applying deconvolved motion. It was determined that the local site condition was accountable for damage severity specially in Fooladi area*

**Keywords:**
Site Effects; Damage Distribution; Earthquake; Sarpol-e Zahab

## 1. Introduction

It is well established that the earthquake ground motion in a specific area is affected by three main factors: the source, the path and local site condition [1]. In general, seismic waves get attenuated as they travel farther from the source. In some cases, site amplifications over soil sediments during strong ground motions cause severe damages, even though the sources are far from the influenced areas. The event of Michoacan that hit Mexico City in 1985 in a distance of 350 Km was a milestone in geotechnical earthquake engineering to understand the behaviour of sediments under seismic motion [2].

Accordingly, the local geology and geotechnical specifications can affect the motion characteristics such as domain, frequency and duration of strong ground motion. It is explicit that during an earthquake, not only source and path are components of surface ground motion intensity and damage level severity, but also the mechanical specifications of the underground layers as well as the geometrical characteristics of the surface (topographic effects) and site subsurface condition are accountable, which is known as site effects today.

In November 12, 2017 an earthquake with magnitude of 7.3 occured in west of Iran and continued for 30 seconds, leading to catastrophic damages to Sarpol-e Zahab city, specially Fooladi area (Figure 1). The largest acceleration caused by the strong ground motion was recorded at

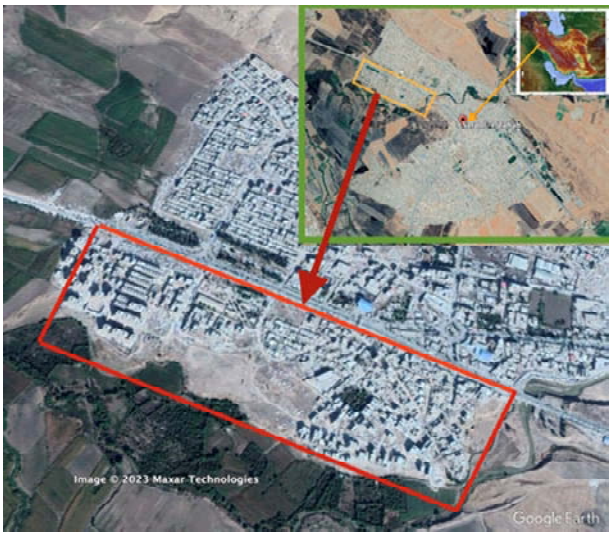


**Figure 1.** Map of Iran and Sarpol-e Zahab, Fooladi area.

Sarpol-e Zahab station (0.69 g in L-component and 0.55 in T-component, Figure 2 [3]) leading to severe damages to a vast area of the city, specially Fooladi area and nearby vicinity (Figure 3). Following a through field investigation right after the earthquake, Moosavi et al. [4] reported that site condition is the first influencing factor on damage distribution all around the city. In the report, it is mentioned that ground surface at Fooladi and Shiroodi area was covered with loose fill material, leading to amplification of the seismic waves. The site effect, in adition to the weak design and construction of the buildings in Fooladi area and its surrounding, exacerbated the destrucion.

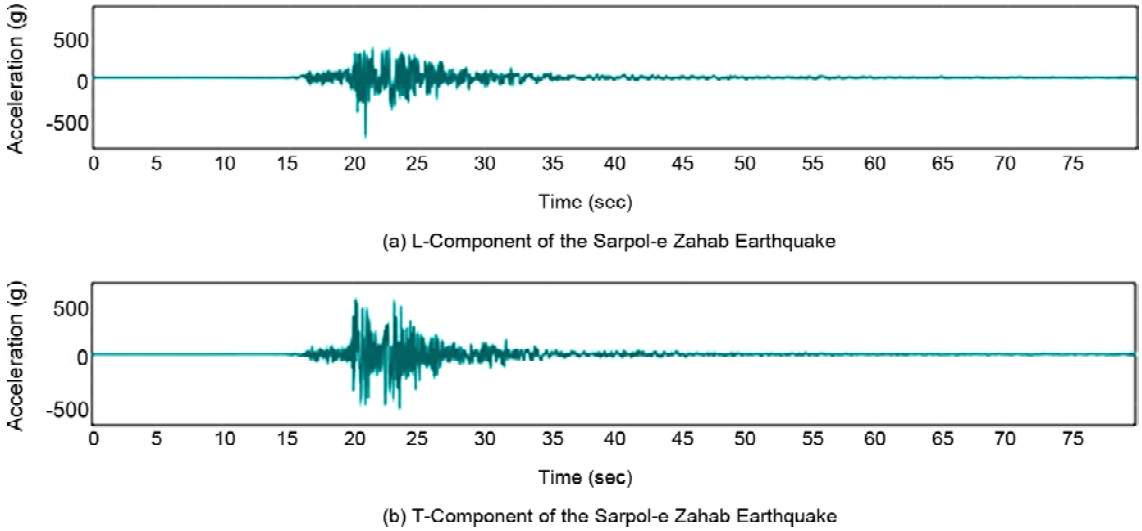


**Figure 2.** components of the Sarpol-e Zahab earthquake reported by the building and housing research center [3].

**Figure 3.** Damaged structures in Fooladi area.

After the event, geotechnical and geophysical survey was conducted on different spots of Sarpol-e Zahab by some organizations such as the International Institute of Earthquake Engineering and Seismology (IIEES), to probe site response analysis. The city ground was classified into different zones based on frequency characteristics, as depicted in Figure (4), which shows the propsed information on natural frequency of the ground in the Sarpol-e Zahab city, prepared by Moosavi et al. [5]. Due to absence of any recorded bedrock motion of the event and its importance to pursue additional studies, Moosavi et al. [6] deconvolved the recorded motion of surface to the seismic bedrock in order to calculate bedrock motion, to be applied at the bottom of the soil profiles to analyze the site response in west of Sarpol-e Zahab. In another research, Zafarani et al. [7] employed the main recorded motion of the surface to perform site response analysis. Ashayeri et al. [8] investigated the effect of shear wave velocity of the soil deposit in upper 30 m of the soil ($V_{30}$) by conducting ambient vibration analysis. Sharafi and Raeisi [9] conducted site two-dimensional numerical simulation and site response analysis using non-linear approach to provide sufficient data for engineers to reconstruct damaged buildings and future construction.

In this study, site condition and the influence of site effects on intensifying the damages in Fooladi neighborhood were investigated according to the significance of site response analysis in that area, following up the previous research of Moosavi et al. [5] in which they produced the map of seismic site classification reffering to surface geophysical exploration and microteremor measurement.

## 2. Methodology

Accelerogram of Sarpol-e Zahab earthquake was recorded by the Building and Housing Research Center (BHRC) seismograph station on the surface of the ground [3]. Epicenter of that event was located on 34.88 northern latitude and 45.84 eastern longitude. Focal depth of this event was estimated about 18 km [10].

To conduct the site response analysis, recorded motion of the surface during the shaking time was employed to produce bedrock motion by applying deconvolution scheme. Site response analysis was perfomed at three locations of the mentioned region (Figure 5). The representative geotechnical profiles were defined by taking into account the data of the geophysical survey by Moosavi et al. [6] and available geotechnical data of other resources after the event [11].

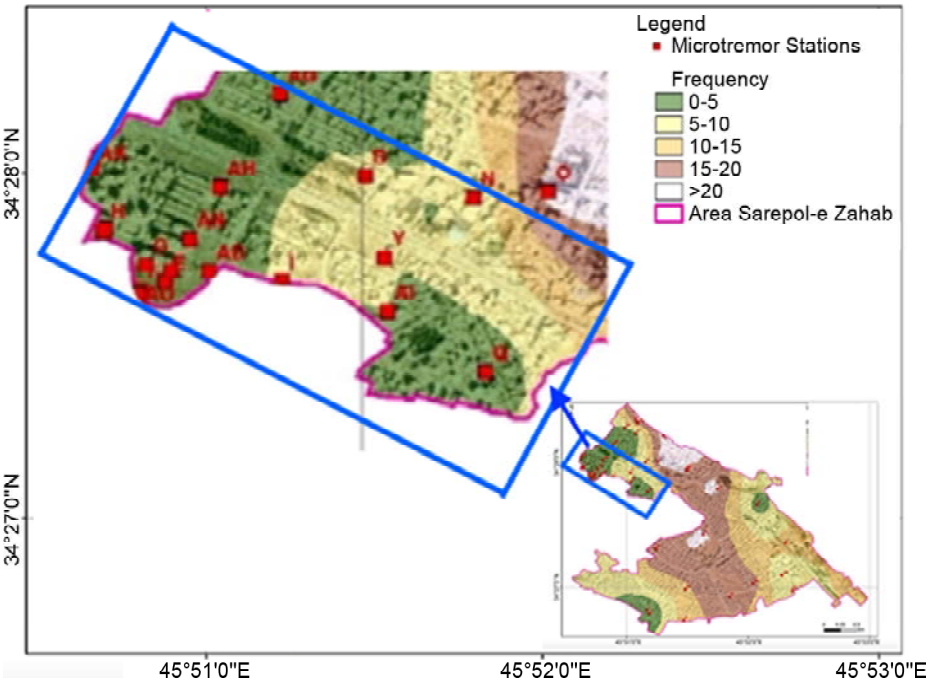


**Figure 4.** Distribution of natural frequency of the soil deposit in Sarpol-e Zahab, zoomed in Fooladi area [5].


**Figure 5.** Location of representative stations preferred for this study.

In this study, field observation reports and aerial photo studies were reviewed and the geotechnical and geophysical data of the afore-mentioned area were collected and examined. Some of examined sites with reliable and available data were chosen to be represntative profiles of the region, in subsequent site response.

### *2.1. Geology of Sarpol-e Zahab*

Map of Sarpol-e Zahab reveals that the city is bound by mountains of Asmari formation at north and north-east. Furthermore, Alvand river crosses the city from the north to the west. Rivers flowing through broad flat valleys have often flooded over neighboring banks periodically. When this occured, the stream velocity quickly decreased, and the gravel and sand particles dropped out in the vicinity of the bank, surounded by remaining finer soils. Consequently, the city is covered by various thicknesses of Quaternary coarse to fine alluvial (Figures 6 and 7)[2].

### *2.2. Field Observation*

A short period of time after the event, a group of

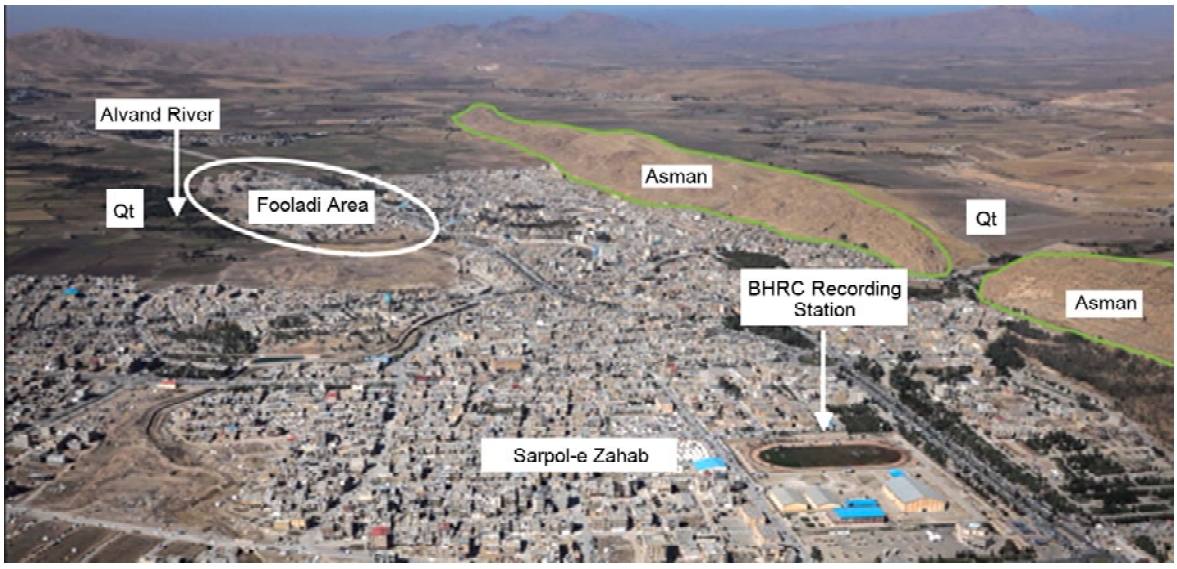


**Figure 6.** Geological Map of Sarpol-e Zahab.


**Figure 7.** Natural soil trenches and alluvial deposits.

**Figure 8.** Sections from the superficial layers of the ground and the built structures over the layers.

researchers visited the affected area and took valuable photos of the whole city. As it is shown in Figure (3), photos represent devastative effects of the earthquake in Fooladi area. In previous researches, it was claimed that buildings were constructed on loose fill material and consequently experienced extra amplification compared to other parts of the city [11]. However, based on the geological condition of the city and field observations, building were located on natural alluvial deposits of fine-grained soil (Figure 8). Although loose fill material existed in some neighboring areas around the Fooladi district, taken photos showed that no building was constructed on those grounds. The satellite imagery of developing hisory of the city from 2007 to 2017 illustrated that the buildings were constructed on agricultural lands (Figure 9).

### *2.3. Data Aquisition and Proccessing*

IIEES employed seismic refraction method to provide sufficient data of soil structure in Sarpol-e Zahab (Figure 10). By using this method, identification of subsurface layering, estimation of thickness of layers and determination of bedrock depth took place [5]. Investigations showed that

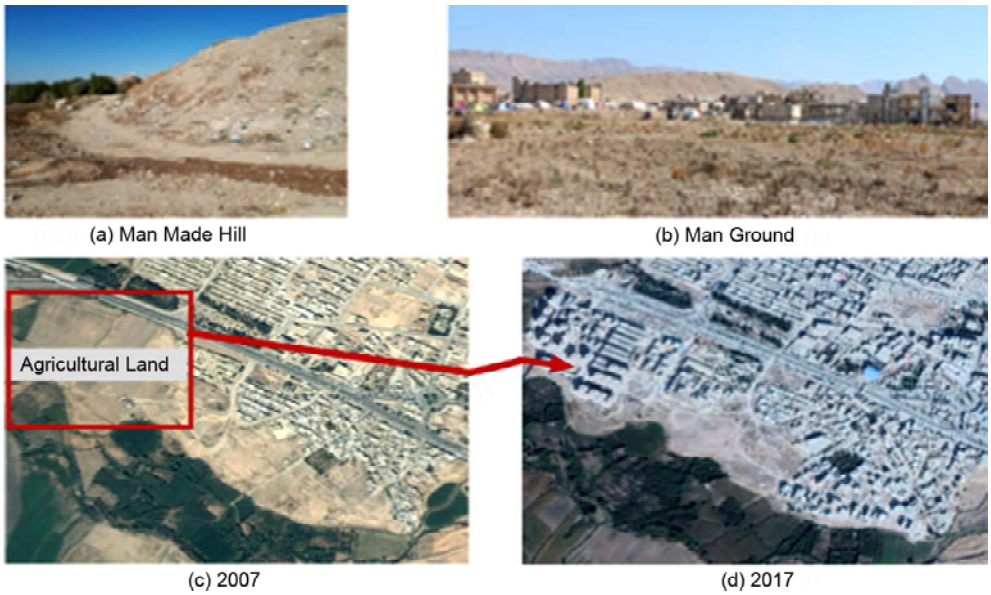


**Figure 9.** (a) Man-made hill, (b) fill material, (c) Satellite imagery of 2007 and (d) Satellite imagery of 2017.


**Figure 10.** Geophysical survey operation at prefered stations for this study.

the thickness of soil deposits increased from the north to the south and the thickness of alluvium was less than 30 m except for some areas near the river. Layering and shear wave velocity in these stations were modeled according to geophysical data. The graph of the shear wave velocity through the depth of each studied point is presented in Figure (11). Regarded to the contrast between shear wave velocity of adjacent layers, site amplification was plausible.

Reports of geotechnical investigations, which were carried out in five areas of Sarpol-e Zahab including Fooladi area were available [11]. The reports contained field and laboratory testings in

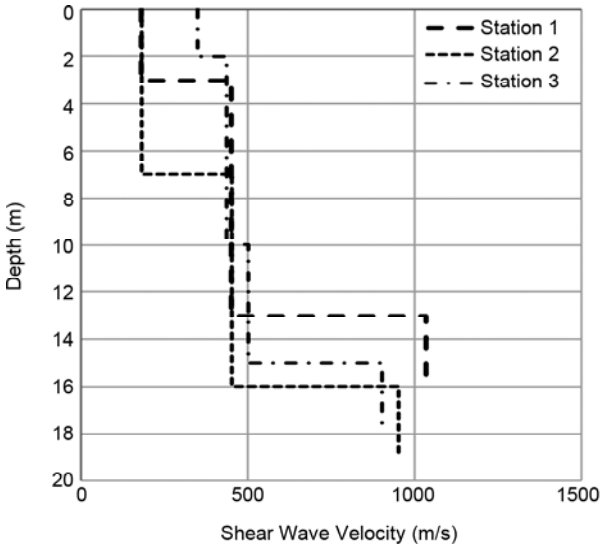


**Figure 11.** Seismic refraction profiles at prefered stations for this study.

**Figure 12.** Location of Geotechnic.

order to identify the subsurface layers of boreholes up to 30 m deep. Figure (12) presents the distribution of geotechnical boreholes and Figure (13) shows the section of these boreholes. In this research, we combined our geophysical data with available geotechnical data at the same place, and produced reliable representatives seismic geotechnical profiles at three preferd locations for this study (Figure 14). Representative profiles mostly contain clay at top elevations and sand at deeper layers. This layering is consistant with field observations by Moosavi et al. within a year after the event (Figure 15) [5-6].

| No | Depth | W.L (m) |
|---|---|---|
| F1 | 30.0 | 12.0 |
| F2 | 30.0 | 14.0 |
| F3 | 35.0 | 13.5 |
| F4 | 30.0 | 12 |
| F5 | 30.0 | 12.5 |

| No | x | y |
|---|---|---|
| F1 | 578290 | 3813794 |
| F2 | 578328 | 3813941 |
| F3 | 578170 | 3813859 |
| F4 | 578305 | 3813718 |
| F5 | 578417 | 3813776 |

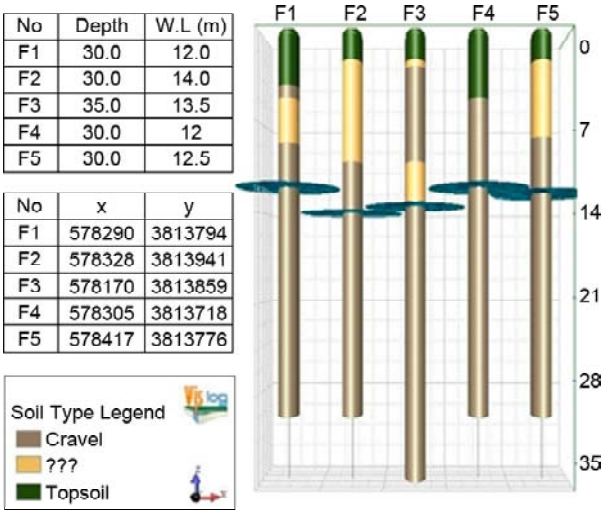


**Figure 13.** Data of geotechnical survey in one of the study areas.

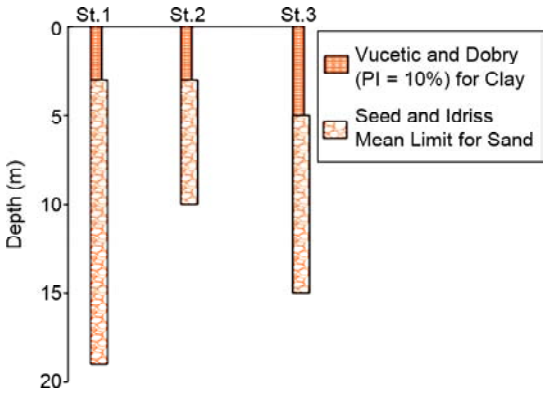


**Figure 14.** Section of representative profiles.

**Figure 15.** Field observations a year after the event.

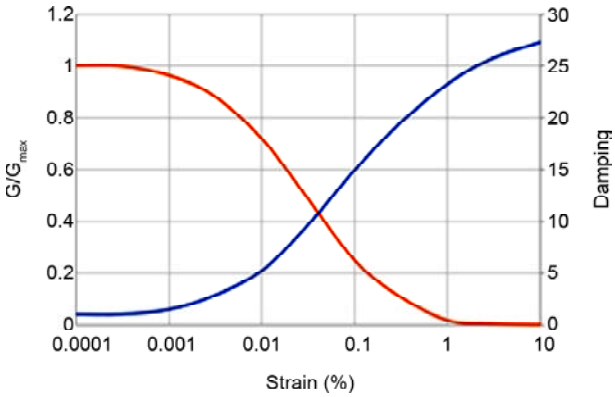


**Figure 16.** Modulus reduction and damping ratio curves used for clay layers in this study.

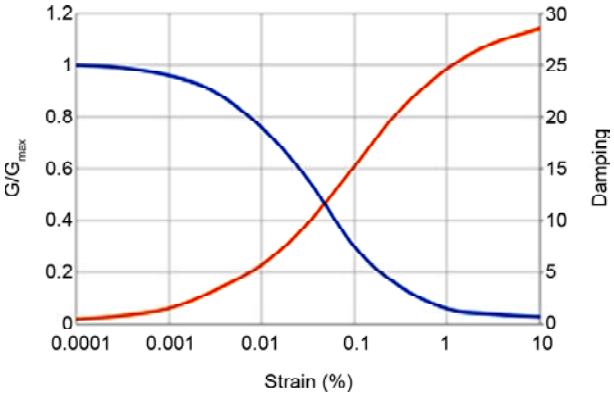


**Figure 17.** Modulus reduction and damping ratio curves used for sand layers in this study.

Based on the above-mentioned data on layering of the representative profiles, clay model proposed by Vucetic and Dobry [12] in 1991 was assigned to top layers, and Seed and Idris [13] modulos reduction curves for sand was also assigned to bottom layers. Curves of modulus reduction and damping ratio variation with shear strain related to the above-mentioned models are presented in Figures (16) and (17), respectively.

### *2.4. Define Seismic Bedrock*

Different criteria are proposed to define seismic bedrock [14]. In geotechnical seismic hazard analyses, proposed by Ishihara and Ansal [15], a medium with shear wave velocity ranging from 600 m/s to 1000 m/s is considered as seismic bedrock. In this study, we followed regultions of the Iranian code of practice for seismic-resistant design of buildings (Standard No. 2800), and considered sublayer with shear wave velocity more than 750 m/s as engineering bedrock [16]. Consequently, the lowest layer of the geotechnical profiles with 1185 m/s shear wave velocity and unit weight of 21 kN/m$^3$ was supposed to be the seismic bedrock.

### *2.5. Computation Bedrock Motion of Sarpol-e Zahab City*

Since the Sarpol-e Zahab time history acceleration was recorded on top of the soil deposits, deconvolving recorded surface motions was necessary to attain bedrock motion. Deconvolution via frequency domain analysis is an effective approach for applying the input motion at any point in the soil column [17]. This method is similar to equivalent linear frequency domain with difference of the input motion location that is on top of the ground [18]. To cross check the results, two different codes, i.e., DeepSoil and SeisGRASP, were utilized to perform deconvolution analyses. SeisGRASP is a site response analysis code based on SHAKE computations [18] and is developed in MATLAB with user friendly graphical interfaces [19]. The input motions can be specified using acceleration time history. SeisGRASP is programmed to evaluate soil response with a given input motion at any desirable depth. It also has some features to process time series. Results of the SeisGRASP are verified by Deepsoil [20-21]. Figure (18) show the Response spectra of the bedrock motion extracted from the SeisGRASP and that of the Deepsoil, by deconvolution of the surface ground motion. As obvious in these figures, results by different codes coincide with each other, which approve reliability of the SeisGRASP.

### *2.6. Site Response Analyses*

After preparation of the representative geotechnical profiles and the bedrock input motions, next step was to perform site response analyses. The site was modeled as a one-dimensional system of horizental and hemogeneous soil layers. Site response analysis was carried out for both L-component and T-component of the calculated bedrock motion at the bottom of each profile as an input motion, by utilizing SeisGRASP in frequency domain, benefiting from equivalent linear method.

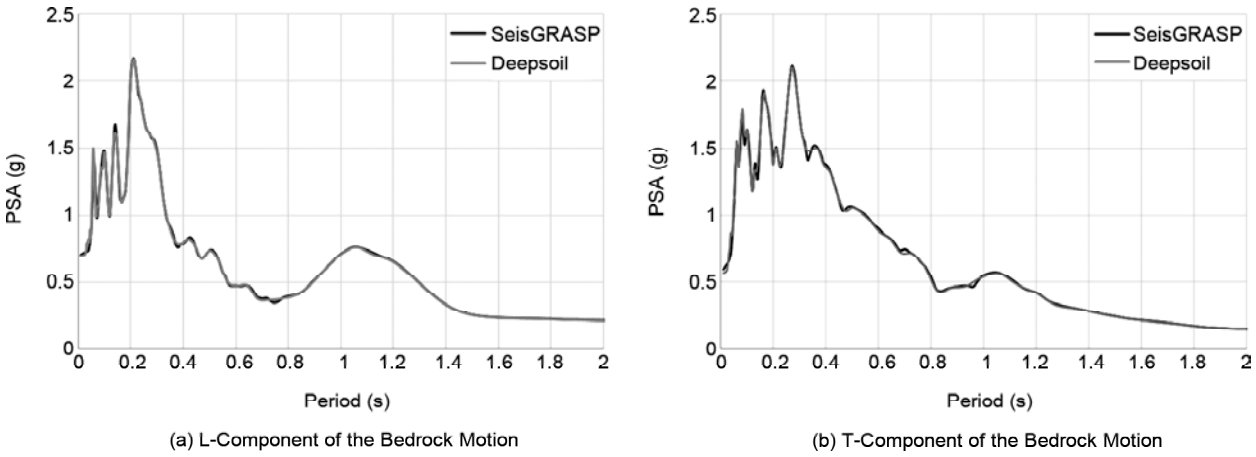


**Figure 18.** PSA Spectrum of the components of the bedrock motion.

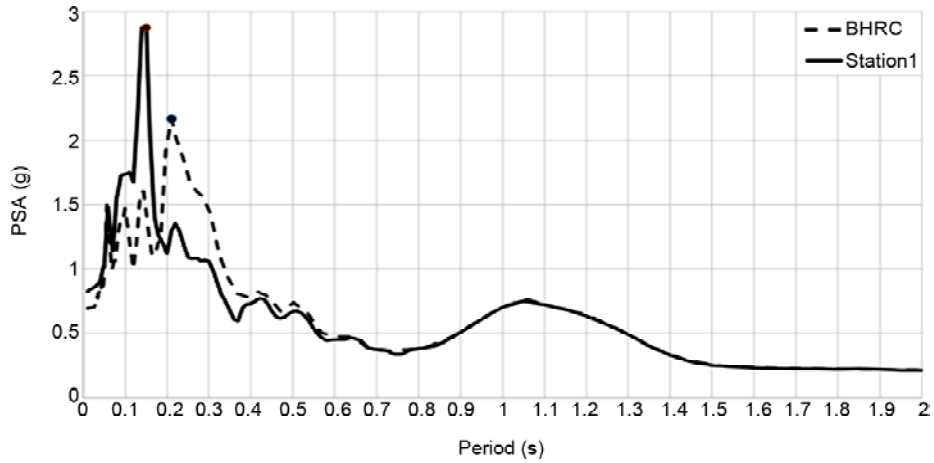


**Figure 19.** Acceleration response spectrum of the L-component of the surface ground motion at Station No. 1.

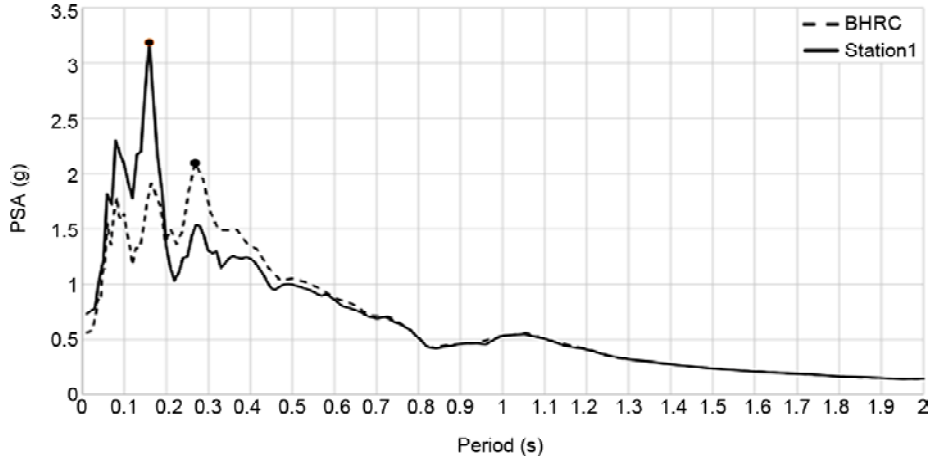


**Figure 20.** Acceleration response spectrum of the T-component of the surface ground motion at Station No. 1.

## 3. Results and Discusions

Figures (19) to (24) represent the pseudo acceleration (PSA) response spectra of the ground surface time histories at each geotechnical profile. In Standard No. 2800 [16], seismic regions are devided into four catagories of risk, i.e., with very low, low, high and very high risk of seismicity. Sarpol-e Zahab was deemed to be of high seismicity, but not predicted to be very intensive [6]. A short period of time after Sarpol-e Zahab earthquake, The United Nations Institute for Training and Research (UNITAR) provided a map for damage

distribution of Sarpol-e Zahab [22]. This map represents the concentration of damages in some areas of the city, including Fooladi area (Figure 25). As it is illustrated in Table (1), the PGA of the site response analyses reached high values up to 0.82 g. Fooladi area was mostly covered with short,

**Table 1.** Calculated PGA at each station by site response analyses.

| Station | L-Component (g) | T-Component (g) |
|---|---|---|
| St1 | 0.82 | 0.72 |
| St2 | 0.63 | 0.73 |
| St3 | 0.65 | 0.74 |

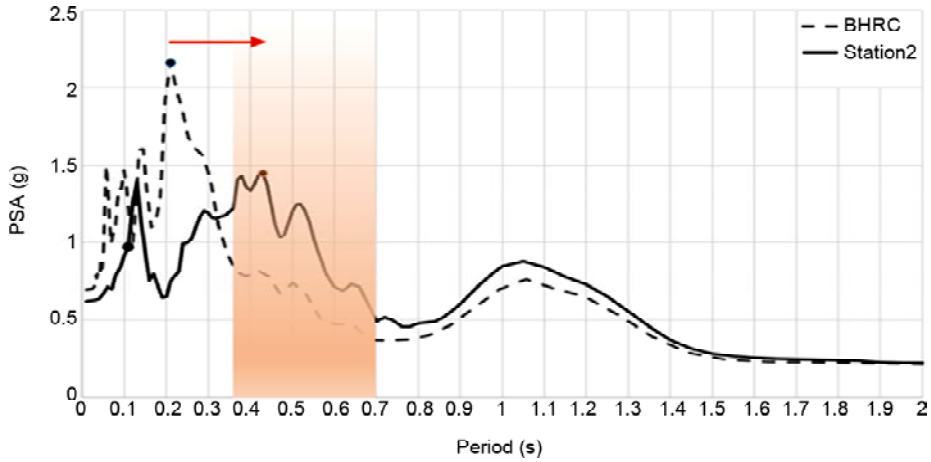


**Figure 21.** Acceleration response spectrum of the L-component of the surface ground motion at Station No. 2..

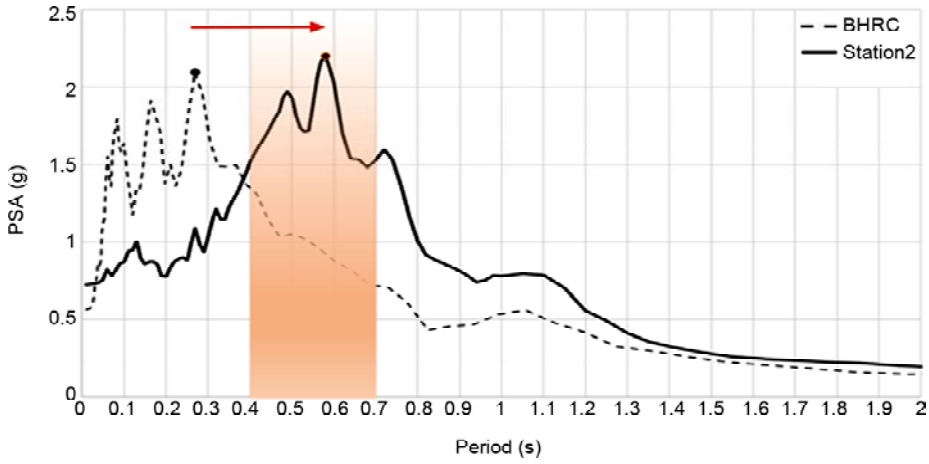


**Figure 22.** Acceleration response spectrum of the T-component of the surface ground motion at Station No. 2.

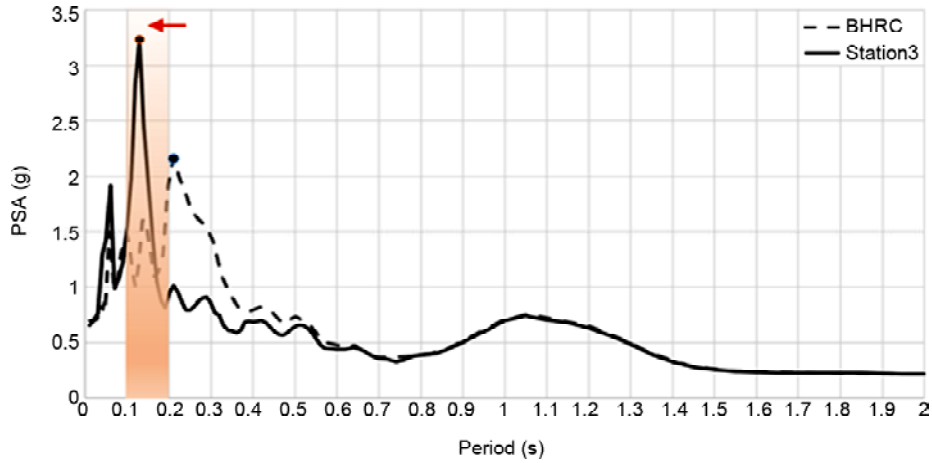


**Figure 23.** Acceleration response spectrum of the L-component of the surface ground motion at Station No. 3.

1 to 2-storey buildings in eastern part and its western part by the name of Shiroodi or Maskan-e Mehr was covered with taller buildings, most of which were the subject of the reported damages in the field (Figure 3). Station No. 1 was located in littoral zone and confirmed there were superficial deposits. PSA spectra represented decreasing value of periods for maximum PSA of station No. 2 to No. 3 from 0.6 s to 0.15 s. Generally, natural period of buildings can be approximately estimated by a simple formula of $T = 0.1\,N$ in which $N$ is the number of stories, so the natural period increases 0.1 s for each story [23]. Regarded to field observation in Shiroodi area 4 to 7-story buildings with 0.4 s to 0.7 s natural periods were severely damaged and in Fooladi area the height of devastated structures declined to 1 to 2-story buildings with 0.1 s to 0.2 s natural periods for which the natural periods of damaged buildings corresponded the PSA spectra results. This resonance of the site and the structures declares the accordance between the damage severity of intensified spots in UNITAR map and the calculated PGA of each station, with evidences observed in the field after the event (Figure 26). It should be noticed that tall building with more than 3 stories were not affected by the earthquake in Fooladi area (Figure 27). Although fill material

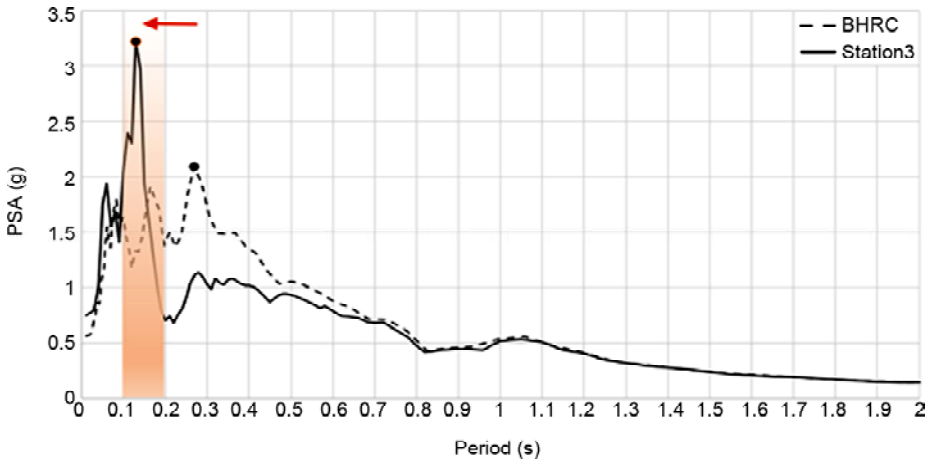


**Figure 24.** Acceleration response spectrum of the T-component of the surface ground motion at Station No. 3.

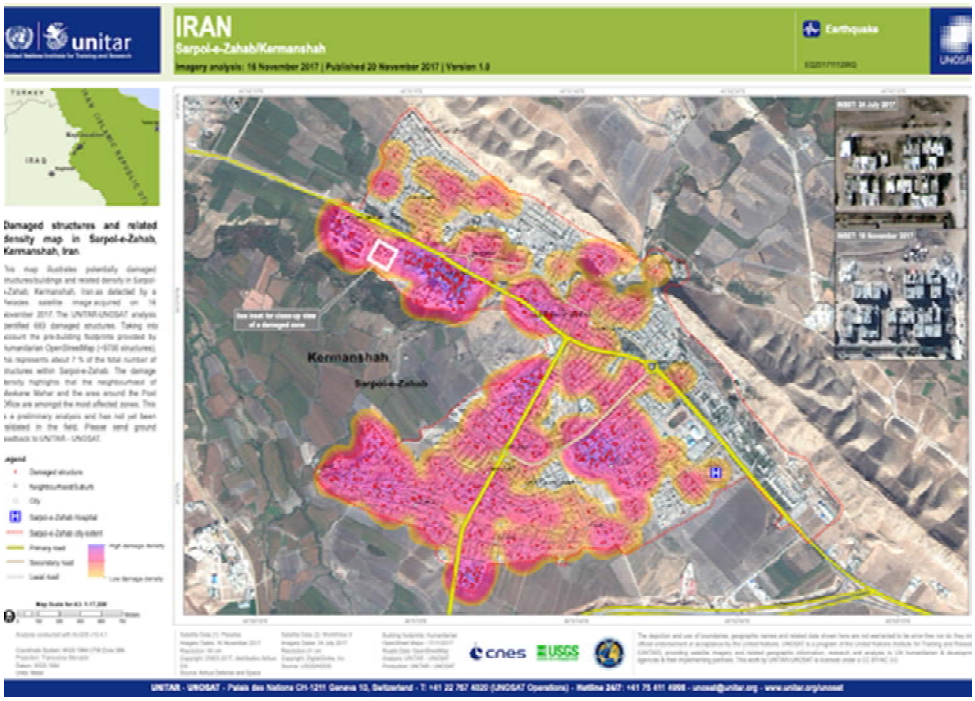


**Figure 25.** UNITAR map of damage distribution [17].


**Figure 26.** Consistency of field observation with UNITAR map.

**Figure 27.** Buildings in eastern part of Fooladi area that survived the earthquake with minor damage.

existed in some areas of the region, it was lack of appropriate seismic geotechnical survey and site effect investigation that led to vulnaribility of the area and caused destructive damages.

## 4. Conclusions

In this research, the effect of local site condition on damage concentration in Fooladi area of Sarpol-e Zahab city was probed. For this purpose, all taken photos of the devastated area and geophysical and geotechnical data were examined precisely. Bedrock motion was calculated by deconvolution of the recorded surface ground acceleration. Site response analyses were conducted subsequently, by employing frequency domain equivalent linear approach to investigate the response of the soil deposit. According to the results of the analyses, peak ground acceleration and response spectra of the surface ground motion were evaluated. Comparison of PGA values and response spectra for each location with UNITAR damage distribution map, illustrated a proper consistency. The conformity of collected data and performed analysis lowered the impact of fill material as the main factor, though it is not negligible. In conclusion, observed evidence indicates that Fooladi region is located on soft soil deposit of sediments and the effect of local site condition over that particular area is confirmed. Short buildings with 2-3 stories are vulnerable to seismic hazards. Lack of geotechnical information of aforementioned region before construction led to dire consequences. Adequate geotechnical study is required in order to provide safe and reliable rehabilitation, reconstruction of affected areas or even the future expansion of Sarpol-e Zahab city.

## References


1. Askari, F., Azadi, A., Davoodi, M., Ghayamghamian, M.R., Haghshenas, E., Hamzehloo, H., and Shafiee, A. (2004) Preliminary seismic microzonation of Bam. *Journal of Seismology and Earthquake Engineering*, **5**(4), 69-80.

2. Chen, Y., Huanng, H., and Wu, C. (2015) Site-effect estimation for Taipei Basin based on shallow S-wave velocity structures. *Journal of Asian Earth Science*, **117**, 135-145.

3. Iran Strong Motion Network (ISMN) Road, Housing and Urban Development Research Center (BHRC), www.bhrc.ac.ir.

4. Moosavi, M., Hahgshenas, E., Ashayeri, I., Tajik, V., Memarian, P., and Zare, M.A. (2017) *Ezgeleh-Sarpol-e Zahab Earthquake Reconnaissance Report (3rd Edition)*. International Institute of Earthquake Engineering and Seismology (IIEES), www.iiees.ac.ir (in Persian).

5. Moosavi, M., Ashayeri, I., Haghshenas, E., Biglari, M., Kamalian, M., and Jalili, J. (2019) Preliminary Seismic Site Classification Map of Sarpol-e Zahab. *Journal of Seismology and Earthquake Engineering*, **20**(4).

6. Moosavi, M., Taleshi Ahangari, H., and Hosseinian, O. (2018) Investigation of site response analyses of the Ezgeleh - Sarpol-e Zahab earthquake, Iran, in West of Sarpol-e Zahab town. *Journal of Seismology and Earthquake Engineering*, **20**(4).

7. Zafarani, H., Jafarian, Y., Eskandarnejad, A., Lashgari, A., Soghrat, M.R., Sharafi, H., and Afraz-e Haji Saraei, M. (2020) Seismic hazard analysis and local site effect of the 2017 Mw 7.3 Sarpol-e Zahab, Iran, earthquake. *Natural Hazard*, **103**, 1783-1805.

8. Ashayeri, I., Memari, M.A., and Haghshenas, E. (2020) Seismic microzonation of Sarpol-e Zahab after Mw 7.3 2017 Iran erthquake: 1D-equivalent linear approach. *Bulletin of Earthquake Engineering*, **19**, 605-622.

9. Sharafi, H., Raeisi, N. (2022) Numerical study of site effects on the amplification of earthquake waves in the fooladi area of Sarpol-e-Zahab city. *Journal of Structural and Construction Engineering*, **8**(6), 97-113.

10. Ashayeri, I., Biglari, M., Sadr, A., and Haghshenas E. (2019) 'Importance of revisiting $(V_s)_{30}$ site class index, Sarpol-e-zahab Mw=7.3 earthquake'. In: *Earthquake Geotechnical Engineering for Protection and Development of Environment and Constructions*, Proceedings of the 7th International Conference on Earthquake Geotechnical Engineering, (ICEGE 2019), Rome, Italy.

11. Islamic Republic of Iran Housing Foundation (2018) *Performance Report and Soil Mechanics Studies in Earthquake-Hit Areas of Sarpol-e Zahab Country*.

12. Vucetic, M. and Dobry, R. (1991) Effect of soil plasticity on cyclic response. *Journal of Geotechnical Engineering*, **117**(1), 89-107.

13. Seed, H.B. and Idriss, I.M. (1970) *Soil moduli and Damping Factors for Dynamic Response Analyses, Technical Repot*. College of Engineering University of California Berkeley, U.S.A., 41p.

14. Shima, E. (1977) On the base rock of Tokyo metropolis. *Proceedings of the 6th World Conference on Earthquake Engineering*, **2**, 433-443.

15. Ishihara, K. and Ansal, A.M. (1982) *Dynamic Behavior of Soil, Soil Amplification and Soil Structure Interaction*. Final Report for Working Group D, UNDP/UNESCO Project on Earthquake Risk Reduction in the Balkan Region.

16. Building and Housing Research Center (2014) *Standard No. 2800 Iranian Code of Practice for Seismic Resistant Design of Buildings*. Fourth Revision, Tehran.

17. Khazaei Pour, M. and Zerva, A. (2018) Efficient time-domain deconvolution of seismic ground motions using the equivalent-linear method for soil-structure interaction analyses. *Soil Dynamics and Earthquake Engineering*, **112**, 138-151.

18. Sooch, G. and Bagchi, A. (2014) A new iterative procedure for deconvolution of seismic ground

motion in dam-eeservoir-foundation systems. *Journal of Applied Mathematics*, Article ID 287605.

19. Idriss, I.M. and Sun, J.I. (1992) *User's Manual for SHAKE91, A Computer Program for Conducting Equivalent Linear Seismic Response Analyses of Horizontally Layered Soil Deposits*.

20. Jalili, J., Moosavi, M., and Pakniat, S. (2022) *Generation and Development of a Comprehensive Site-Response Analysis Code in Time and Frequency Domain - Part 1: Frequency Domain Analysis*. Research project fulfilled at the International Institute of Earthquake Engineering and Seismology.

21. Hashash, Y.M.A., Musgrove, M.I., Harmon, J.A., Groholski, D.R., Phillips, C.A., and Park, D. (2016) *DEEPSOIL 6.1, User Manual*.

22. United Nations Institute for Training and Research, Satellite image and analysis (2017) *Maps and Data*.

23. NBCC (1995) *National Building Code of Canada*. National Research Council of Canada, Canadian Commission on Building and Fire Codes.